Antenna Pointing Systems for Large Communications Satellites

J. Broquet,* B. Claudinon,† and A. Bousquet†
Matra Space Branch, Velizy Villacoublay Cedex, France

Most of the geostationary satellites already developed operate antenna pointing through fine orientation measurement and control of the satellite main body to which each antenna is rigidly attached. The main body orientation is measured by means of infrared Earth observation. Increasing antenna size and power and, sometimes, political constraints enhance the benefit of very accurate antenna pointing (0.05 deg, 3 σ at antenna electrical axis level). This typically implies direct measurement of antenna orientation through the use of radio-frequency sensors incorporated in each antenna, mechanical decoupling between antennae to allow for compensation of structural deformations, and mechanical decoupling between each antenna and the satellite main body through the use of antenna pointing mechanisms to allow for high antenna control bandwidth. Concepts of antenna pointing mechanism and associated control for such satellites are presented shortly. Pointing performances of attitude control concepts alternatives are shown for a typical payload.

Introduction

THE evolution of satellite communications towards complex multibeam systems as well as the increasing payload capabilities and size make distributed attitude control concepts more and more attractive. Each beam could be pointed independently through antenna pointing mechanisms and radio-frequency sensors. When deriving attitude control concepts, satellite designers now must trade against the use and number of antenna pointing mechanisms and radio-frequency sensors.

Approaches to antenna pointing and main body orientation are first presented and discussed. The need for radio frequency sensors (RFS) and antenna pointing mechanisms (APM) is expressed as a function of the antenna number and individual pointing accuracy. RFS is implemented in the antenna to be pointed and thus materializes its radio-frequency boresight. No more error is involved between a main body sensor, e.g., an infrared Earth sensor (IRES) and the antenna. RFS principles and characteristics are briefly reviewed.

Several APM mechanization control concepts are proposed. The selection of an APM and a control concept is highly dependent on the mission. The important parameters for a choice are the antenna size and structure (flexibility), the required offsetting capability, the mechanical interface between the antenna and the main body, and the main body pointing capability. Alternatives to the antenna control are developed and simulations results are shown.

Lastly, different spacecraft configurations making use of RFS and APM or not, are elaborated for a given payload. Pointing budgets are derived from simulation and analysis results for each antenna, outlining the effects of the aforementioned selection parameters.

Antenna Pointing Control Problem

Satellite Body Attitude Control

The design of attitude control systems for three-axis stabilized geostationary satellites is strongly governed by the problem of long-term yaw control. Continuous yaw control systems from direct yaw sensing, through the use of star sensors or combination of gyros and sun sensors, are penalized by the implementation and reliability problems, respectively. Radio-frequency sensors are at an early stage of development and presently do not offer accurate yaw measurement capability. Thus, yaw control from roll/yaw coupling through the use of satellite internal angular momentum still appears the simplest solution for the telecommunications satellites of the eighties.

Illustrations of geostationary satellite attitude control with fixed momentum wheel and with typical skewed momentum wheels are respectively shown in Figs. 1 and 2. See also Ref. 1.

Fixed Momentum Wheel (Fig. 1) [1 Degree-of-Freedom (DOF) System]

Earth sensor provides angular attitude measurement about the $X(\varnothing)$ and $Y(\theta)$ axes but not about the Z-axis (ψ angle).

Roll angle and nutation are simultaneously controlled through an adequate firing sequence of skewed X/Z thrusters. The inherent coupling of roll into yaw due to the orbital motion results in a yaw maximum error over the orbit which depends only on momentum bias, disturbing torques, and roll control deadband.

Two-Degree-of-Freedom (2 DOF) Momentum

Improvement of the 1 DOF control principle can be achieved through transverse momentum generation capability, either via a gimballed wheel, an additional reaction wheel, or as described hereafter by using two skewed momentum wheels (Fig. 2).

The angular momentum H can be moved inside the satellite within the wheel plane (H_1, H_2), (YZ plane on the figure). Linearized attitude control can be obtained about the axis perpendicular to the wheel plane, thus improving the control accuracy.

Attitude control about roll (X) axis and pitch (Y) axis is performed by wheel speed command. [Roll (X), pitch (Y), and yaw (Z) axis are along East-West, North-South, and satellite-Earth directions, respectively.] Signal processing is defined to minimize satellite attitude transients under Earth sensor noise effect and satellite disturbance effect. Yaw control is still operated through skewed X/Z thruster actuation to maintain the mean orientation of the satellite angular momentum. Several other possibilities will certainly be offered to new geostationary satellites. Current studies could prove the capability of some gyro technologies to meet the reliability requirement for long-lifetime missions. (See Ref. 2, 3, and 4).

Presented as Paper 82-0444 at the AIAA 9th Communication Satellite Systems Conference, San Diego, Calif., March 7-11, 1982; received April 1, 1982; revision received Jan. 27, 1984.

*Senior Engineer, Head of Advanced Studies Department.
†Senior Engineer, Advanced Studies Department.

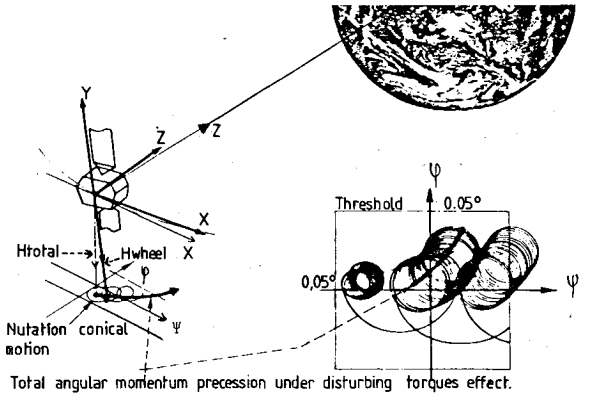

Fig. 1 Geostationary satellite with fixed momentum wheel; principle of roll-yaw control in normal mode.

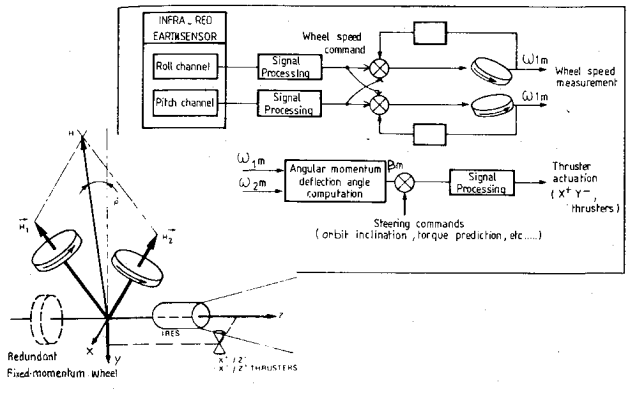

Fig. 2 Geostationary satellite with typical skewed wheel configuration; attitude control principle.

Need for RF Sensing and Roll/Pitch Controls

More specific is the problem of meeting a very high pointing accuracy requirement, typically 0.05 deg half-cone angle during nominal satellite operations, at antenna beam axis level.

Attitude measurement from infrared Earth sensing will not meet such a requirement because all structure distorsions (thermal, hysteresis, aging, initial alignment uncertainties) between the IR sensor and the antenna axis penalize the pointing performance, and since the antenna beam deviation caused by the yaw error cannot be observed through the IRES, a very accurate sensor (radio-frequency sensor), stiffly associated with each of the antennae to be controlled, must be used for individual antenna pointing detections.

Alternate Solutions and the Need for Antenna Pointing Mechanisms

Roll-pitch antenna control can be obtainted through electronic antenna beam deflection, and mechanical decoupling between satellite sub-elements, namely the antenna/satellite main body and the antenna attached to the satellite main body/internal angular momentum (momentum wheel gimballed around roll axis or multiple fixed-momentum wheel in pitch/yaw plane).

Satellite attitude control alternatives differ according to the number of payload antennae supporting RF sensors and requiring very accurate pointing. Attitude control system (ACS) actuator concepts for a payload with a single high accuracy antenna are typically: a) 2-DOF system (two-wheel configuration of single-gimballed momentum wheel) for the attitude control of the whole satellite, b) 3-DOF system (multiple wheel configuration or double-gimballed momentum wheel) for the attitude control of the whole satellite, c) 1-DOF system and one-axis antenna pointing mechanism (APM) controlled in closed loop with large bandwidth, and d) 1-DOF system

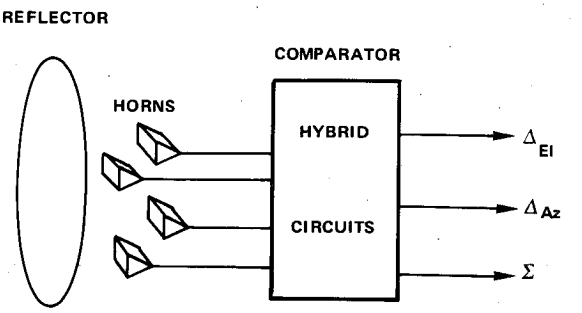

Fig. 3 Multilobe technique.

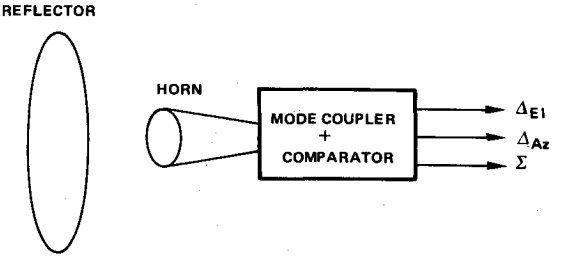

Fig. 4 Multimode technique.

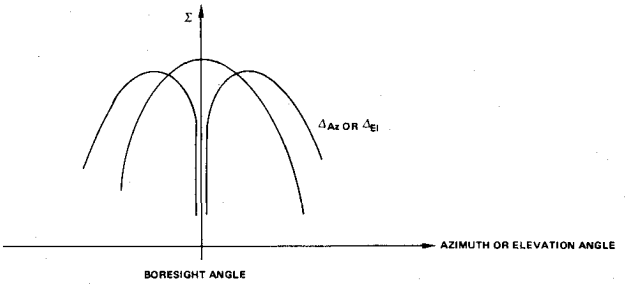

Fig. 5 Signal patterns.

and two-axis APM controlled in closed loop with large bandwidth.

ACS actuator concepts for a payload with several high-accuracy antennae necessarily include antenna pointing mechanisms, whether combined or not with linearized roll-pitch control of the satellite main body. At a minimum, the APM function is to eliminate the structural bias and distortion between the antennae and main body. In this case, only low-bandwidth (LBW) actuation capability is required (low bandwidth APM).

The other APM functions are related to high-bandwidth (HBW) control. They are accurate high-bandwidth angular control of the individual antenna beam orientation and high bandwidth control of the linear antenna motion to avoid internal antenna vibrational deformation (very large antenna only).

RF Sensing

RF sensing development efforts are based mainly on two principles depending on the horns utilized to receive the ground beacon signal. These are:

1) Multilobe (Fig. 3), in which separated horns (typically four) receive signals for which the phase difference is a function of the antenna pointing w.r.t. the beacon direction. Elevation (Δ_{El}) and azimuth (Δ_{Az}) signals are obtained after a proper combination (comparator) of the horn signals through hybrid circuits as well as the sum (Σ) signal used as a reference.

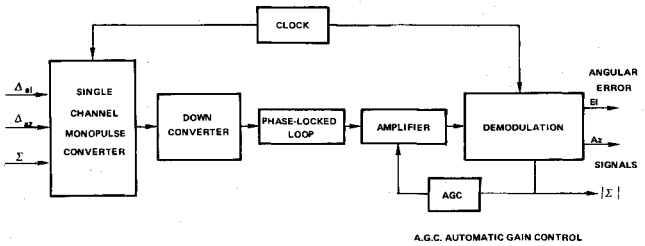

Fig. 6 RFS signal processing.

Table 1 Typical field-of-view and accuracy

Frequency, GHz	F.O.V. (reflector diameter $d = 2$ m), deg	Accuracy, deg
6	1.75	< 0.050
14	0.75	< 0.020
20	0.525	< 0.015

2) Multimode (Fig. 4) in which a corrugated horn is used for which wave higher order modes are excited when the boresight axis is not aligned with the beacon direction. The dominant mode is equivalent to the signal and the higher order modes in orthogonal planes correspond to Δ_{Az} and Δ_{El} with identical patterns (Fig. 5). Extraction of the modes is done through a mode coupler and elaboration of Δ_{Az} and Δ_{El} again through a comparator.

Signal processing, shown in Fig. 6, is common for the two types of sensors. It yields a sum ($|\Sigma|$) voltage which can serve as a beacon presence signal and two error (El, Az) voltages proportional to the angular pointing errors.

The practical limitations of the radio-frequency sensor are essentially, as seen in Table 1: a) its field-of-view; if no special treatment is made, it is equivalent to the antenna 3 dB aperture; b) its noise level, depending on the beacon emitting power, the processing electronics, and on the required bandwidth; c) its sensitivity to structural problems. It could be crucial if horns and reflector are not rigidly linked, e.g., horns on the main body and reflector offset by a mast.

Antenna Pointing Mechanisms

The purpose of this section is to review the main principles of APM mechanization and to show their limitations and interests. As a matter of fact, the choice of the APM type is strongly related to the control objectives and, therefore, a proper optimization of this mechanization may decrease the control problem complexity, saving time, cost, and mass.

Main Principles

Several concepts of APM have already been derived in many space firms. Some of them are now under development or qualification. The APM's are defined to move part of the antenna (reflector) or the whole antenna, according to the antenna type (central feed, offset) and size. APM concepts differ in terms of rotation axis location (real or virtual axis), pivot mechanization, motor type and drive, and resolver (orientation measurements).

Type 1: Gimbal-Based Antenna Pointing Mechanism Concepts

Conventional APM's are derived from previous works performed on gimballed momentum wheels. They generally use ball bearing and either stepper or DC motors about each axis (Fig. 7). Similar mechanizations are proposed for APM's with flexural bearings. The advantage of this mechanization is to allow large angle deflection, but the total mass is generally important.

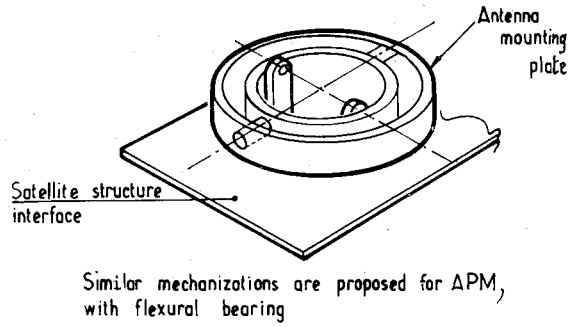

Fig. 7 Principle of APM using gimbals.

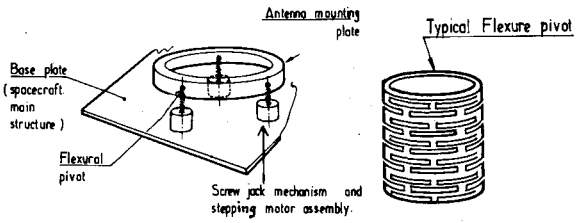

Fig. 8 Principle of pivot-based APM.

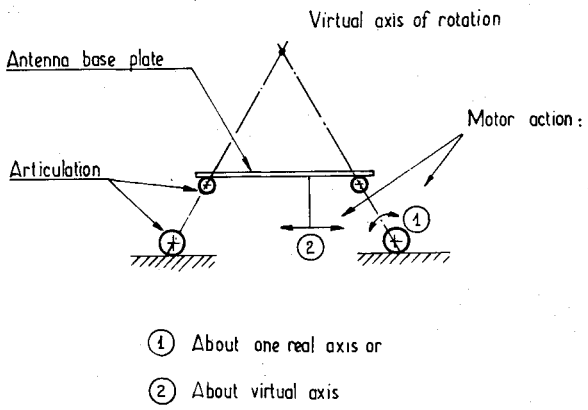

Fig. 9 Principle of a one-axis APM providing rotation about virtual axis (for small angle only < 3 deg).

Type 2: Pivot-Based Antenna Pointing Mechanism Concepts

Conventional pivot-based APM concepts are also derived from previous work on gimballed momentum wheels, in particular, the screw jack and stepper motor mechanization which features full redundancy through symmetrical actuator and pivot arrangement (Fig. 8). Screw jack mechanisms are replaced in some concepts by linear DC motors featuring no contact between movable pieces, but requiring caging for launch.

Type 3

As an extension of type 1 concepts, an APM concept with an additional gimbal is proposed to offer antenna (or sub-part) orientation around virtual axes which can be far away from physical gimbal axes (Figs. 9, 10, 11). This principle can be realized by choosing the blade stiffness such that

$$d_3 = 2d_1 \quad \text{and} \quad d_1 = \frac{\theta_2}{2\theta_1} d_2$$

as shown in Fig. 11.

Such concepts can be applied in either of two cases. When the APM orients only the antenna reflector, the rotations can be performed around the antenna horn and the antenna

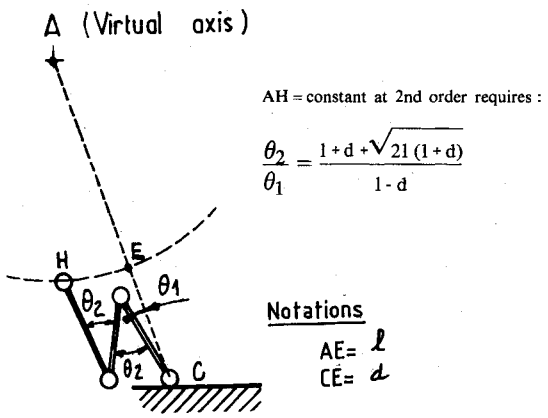

Fig. 10 Principle of articulation for rotation about virtual point.

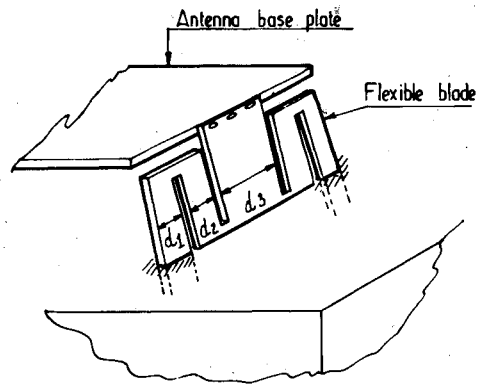

Fig. 11 Flexible blade shaped to generate multiple equivalent rotation axis. Rotation about virtual axis is obtained for angles up to 10 to 15 deg.

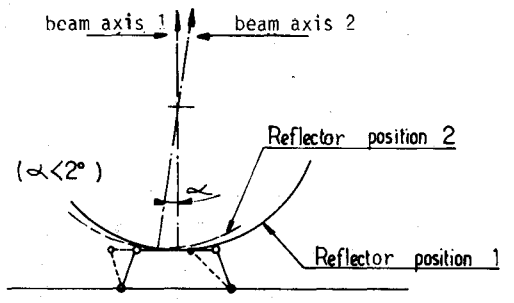

Fig. 12 Application of virtual axis APM to rotate antenna reflector about the horn.

focalization can be maintained within a few degrees, whatever the beam rotation may be (Fig. 12). When the APM orients the whole antenna, the rotations can be performed around the satellite center of mass and dynamical decoupling between antenna and satellite main body can then be optimized according to the satellite configurations.

Type 4

Three biased rotation axes (but close to each other) define a coning motion which can be used to control the antenna pointing (Fig. 13). The three axes are necessary for azimuth and elevation corrections. Very high stiffness and accuracy (< 0.005 deg) can be obtained.

Antenna Orientation Mechanism Implementation

Reflector flexible mode frequencies are expected to be higher by a few Hz than the control bandwidth, and thus need not be

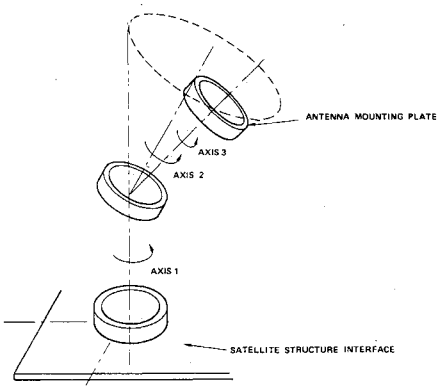

Fig. 13 APM type 4.

CONFIGURATION	COMMENTS
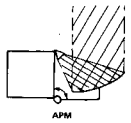	• Excitation of reflector symmetrical modes • Excitation of support structure bending modes • Large load inertia • More adapted to central feed antennae
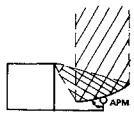	• Small load inertia • Excitation of reflector unsymmetrical modes • Small defocalization due to rotation
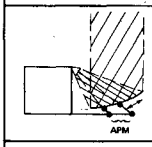	• Virtual rotation about the focal point • No reflector modes excitation • Excitation of support arm modes • No defocalization due to antenna motion
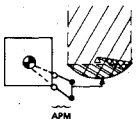	• Virtual rotation about the S/C center of mass • Excitation of reflector and support structure modes • Good isolation w.r.t. the central body rotation • More adapted to central feed antennae

Fig. 14 Influence of APM location and type.

controlled. Therefore, these modes must not be excited in an open-loop manner by the control system.

The choice of the APM location must take into account several criteria: minimization of the reflector mode excitation resulting from APM actuation, isolation w.r.t central body motion, minimization of the load inertia to enable sufficient control bandwidth, and not to induce severe requirements on the actuator itself, and keeping the horns as close as possible to the focal point when the antenna is moving. At a lower level, criteria include minimization of the support structure inertia to avoid very low frequencies and high coupling with the main body and minimization of the antenna support structure mode excitation resulting from the APM actuation.

All these criteria are generally conflicting requirements and the mechanism type and implementation must be optimized in order to minimize the pointing error and/or the control system complexity and weight. The influence of APM location and type is illustrated in Fig. 14.

Antenna Control Through RFS and APM

Two approaches have been explored. In the decentralized approach, an independent RFS/APM control loop is designed separately from the main body control. This approach is valid only when the antenna inertia is sufficiently lower than the inertia of the rest of the spacecraft. In the centralized approach, both main body and antenna are controlled as a

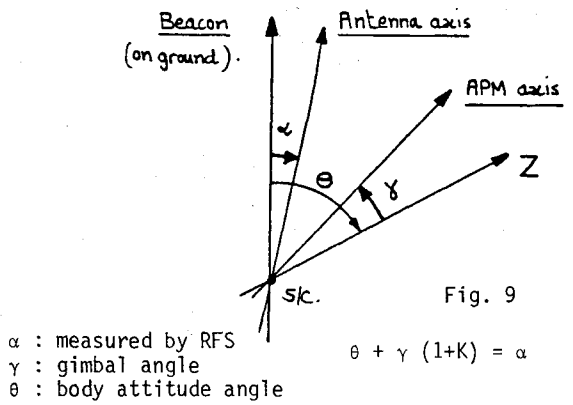

Fig. 15 Relationship between body attitude, gimbal angle, and RFS axis.

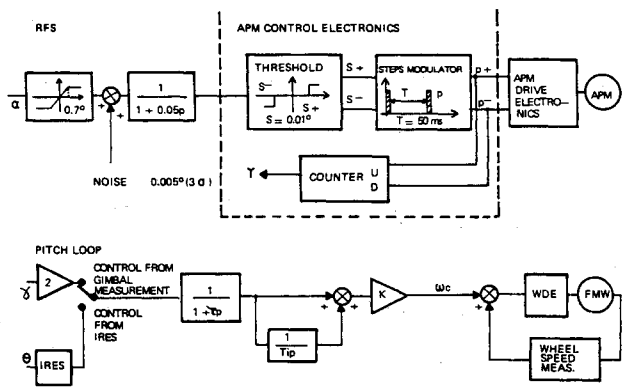

Fig. 16 APM control simplified block diagram.

multivariable system. Modern linear-quadratic (LQ) optimal control techniques are applied. A detailed structural model of the spacecraft must be used.

Decentralized Approach: Independent Antenna Pointing

A large communications satellite with a small antenna is considered. The antenna is mounted on a type 1 APM (as defined in the section covering APM's) using gimbals and stepper motor. The antenna and body control loops are based on simple classical designs and built separately. The antenna control loop uses the APM and the RFS. When the RFS output exceeds a given threshold, steps are ordered via the APM drive electronics. An inhibition time is set between two steps corresponding to maximum APM pointing speed. Typically, the step size (α) is about 0.005° and a step actuation corresponds to an antenna beam axis motion of $(1 + K)\alpha$ where the deviation factor K depends on focal length/antenna diameter ratio (when the APM moves only the reflector and not the feed). Consequently, the threshold S must be at least equal to the beam deviation angle due to one step actuation. A margin for RFS noise effect must be also included. The steps are counted in an up/down counter which gives a gimbal angle measurement, provided that the step size accuracy is sufficient. However, an accurate angle pickoff (resolver) is generally used in order to avoid misstepping effect.

The main body control loop uses the momentum wheel and the gimbal angle pickoff. As a matter of fact, the gimbal angle value γ represents the attitude angle (with a factor $1/(1 + K)$ and assuming that the RFS output is null) as indicated in Fig. 15. Obviously, an Earth sensor, if available, can be used for main body control. A simplified block diagram is shown in Fig. 16. To illustrate the performance of this control scheme,

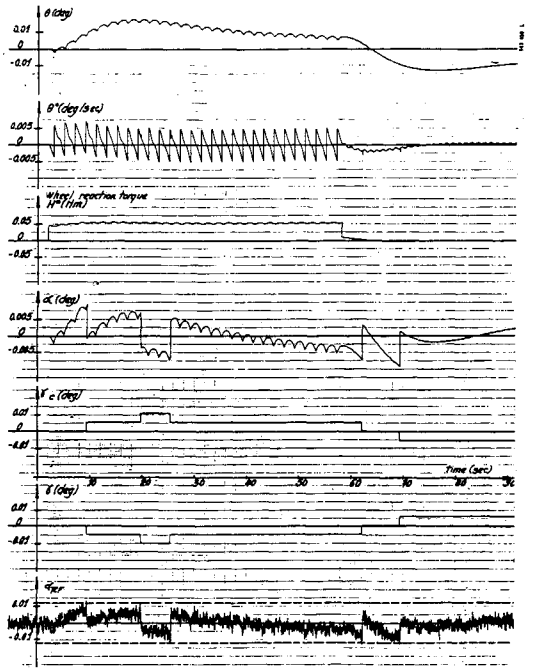

Fig. 17 Momentum unloading simulation showing performance of independent antenna pointing.

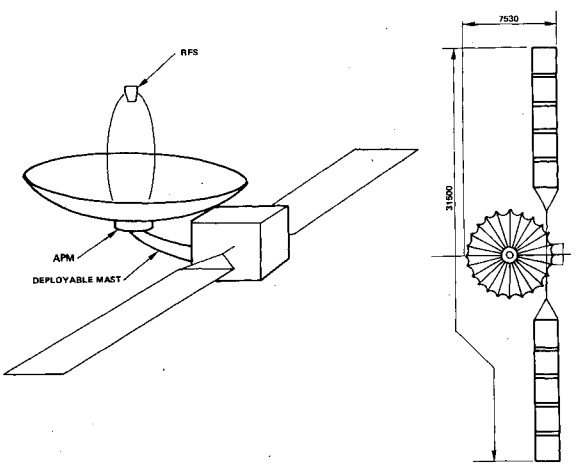

Fig. 18 Satellite configuration.

simulation results on pitch control during momentum unloading are given in Fig. 17. A sequence of 25 Y-thruster actuations (0.1 Nms) is given in open-loop. This simulation takes into account body and antenna inertiae as well as APM model and some solar array flexible modes. Low-level catalytic thrusters are used.

It has been shown that the APM keeps the antenna axis within the deadband (0.01°) during all the satellite operational modes including stationkeeping. Limitation of this technique appears when the antenna inertia cannot be neglected w.r.t the body inertia, and the antenna flexible modes or antenna support system flexible mode are within or close to the system control bandwidth. In these cases, special care must be taken to implement independent antenna control systems and generally a centralized approach must be envisaged.

Centralized Approach: Modern (LQ) Optimal Control

In this approach, an overall modal model of the structure must first be obtained to get all the necessary flexible mode information (see configuration in Fig. 18). A one-axis model is

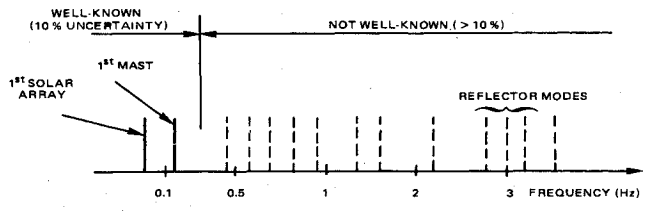

Fig. 19 Typical mode configuration.

represented by:

$$\dot{x} = Ax + B(u + d) \tag{1}$$

$$y = Cx \tag{2}$$

where

$$x^T = (q1, q2 \ldots qn, \dot{q}1, \ldots \dot{q}n) \tag{3}$$

$q1$ = rigid body mode variable

$q2, \ldots, qn$ = flexible mode variables

$$u^T = (u1, u2) \tag{4}$$

$u1$ = main body control variable (thruster torque)

$u2$ = APM control variable

$d^T = (d1, 0)$ = disturbance torque

$$y^T = (y1, y2) \tag{5}$$

$y1$ = main body sensor measurement (IRES)

$y2$ = RFS measurement

The active controller consists of a state observer

$$\begin{cases} \hat{x}_k = \hat{x}_{k/k-1} + L(y_k - C\hat{x}_{k/k-1}) \\ \hat{x}_{k/k-1} = F\hat{x}_{k-1} + Gu_{k-1} \end{cases} \qquad k = 0, 1 \ldots \tag{6}$$

where $\hat{x}_k$ is the estimated state at time k, and F and G are the discretized form of A and B, and of a state feedback

$$u_k = K\hat{x}_k \tag{7}$$

The state dimension ($2n$) is usually very large. Due to mode uncertainties (Fig. 19), performance and stability considerations, it is necessary to reduce the controller order.[5-8]

Note that this approach is very favorable to a priori identification of the disturbance d. Figure 20 shows the results obtained for the previous structure (1,800 kg, six flexible modes) during stationkeeping. Three modes are controlled. Disturbance (1 Nm) is assumed known with 10% uncertainty and main body control is performed by 10 Nm thrusters (bipropellant).

Table 2 Main error types and values

Type	Roll	Pitch	Yaw
	(3 σ, deg)		
Initial alignment			
RF boresight axis vs geometrical axis	0.02	0.02	0.1[a]
antenna reference vs body reference	0.02	0.02	—
momentum wheel vs body reference	—	—	0.03
momentum wheel vs IRES	—	—	0.01
Alignment stability			
Antenna/IRES			
Bias	0.022	0.022	—
Thermal distortion	0.018	0.018	—
Wheel/antenna			
Bias	—	—	0.04
Thermal distorsion	—	—	0.04
Wheel/IRES			
Bias	—	—	0.05
Thermal distorsion	—	—	0.04
IRES			
Constant errors			
Alignment	0.01	0.01	—
Bias between roll/pitch channels	0.011	0.011	—
Short-term variations	0.05	0.05	—
Long-term variations:			
Seasonal effect (residual errors)	0.012	—	—
Meteorological effect (residual errors)	0.022	0.018	—
Aging	0.023	0.023	—

[a] Polarization

Comparison of Typical Antenna Pointing Performances

Selected Example

A satellite consisting of a rigid main body with symmetric solar panels and three communications antennae is considered. One antenna is rigidly connected to the main body and the reflectors of the other two are either fixed or mounted on an APM. Body actuation is either a 1 DOF (1 momentum wheel) or a 2 DOF (2 skewed momentum wheels) concept.

Error Sources and Budget

The different error sources are classically identified according to sensors, equipment misalignments, structural deformations, and control. Disturbances (actuator non-linearities and imperfections) flexibilities, and sensor noises are taken care of by the control and their effects are evaluated in the so-called control error type. Our main assumptions are listed in Table 2.

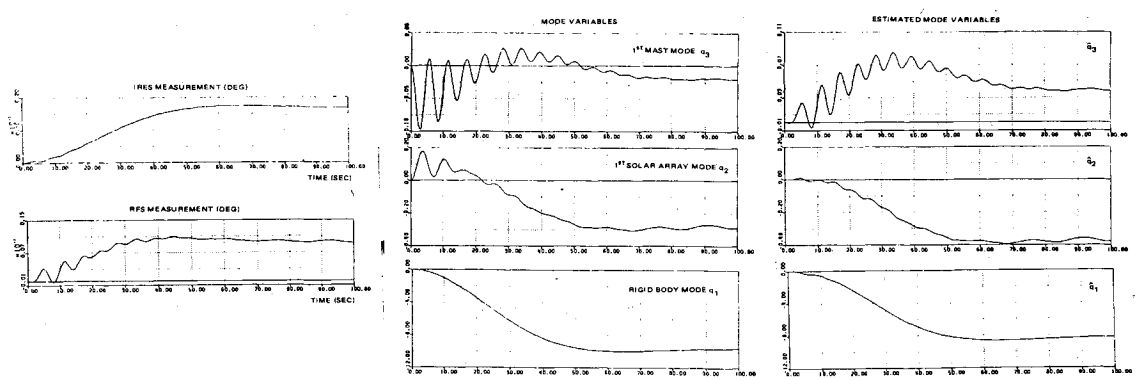

Fig. 20 Centralized approach simulation results.

Table 3 Normal mode error budget for each antenna

Configuration	Large antenna, deg	Offset antenna, deg	Fixed antenna, deg	Body control
I	RFS, 0.053	0.105	0.105	RFS 2 DOF
IIa	RFS, 0.073	APM (LBW)[a] 0.098	0.132	RFS 1 DOF
IIb	RFS, 0.053	APM (LBW)[a] 0.096	0.105	RFS 2 DOF
III	Calibration, 0.097	APM (LBW)[a] 0.097	0.129	IRES 2 DOF
IV	RFS + APM (HBW)[b] 0.043	APM (HBW)[b] 0.081	0.132	RFS 1 DOF

[a]LBW = Low Bandwidth [b]HBW = High Bandwidth

Table 4 Station-keeping mode error budget

Configuration	Large antenna, deg	Offset antenna, deg	Fixed antenna, deg	Body control
I	RFS, 0.119	0.169	0.169	RFS 2 DOF
IIa	RFS, 0.118	APM (LBW)[a] 0.149	0.178	RFS 1 DOF
IIb	RFS, 0.119	APM (LBW)[a] 0.151	0.169	RFS 2 DOF
III	Calibration, 0.163	APM (LBW)[a] 0.163	0.193	IRES 2 DOF
IV	RFS + APM (HBW)[b] 0.043	APM(HBW)[b] 0.09	0.178	RFS 1 DOF

[a]LBW = Low Bandwidth [b]HBW = High Bandwidth

All error values are given for a probability level of 0.9974 (3 σ). In order to combine them, they are classified into four categories according to their time characteristics: class A, constant errors; class B, low-frequency errors with a period greater than or equal to 24 h; class C, high-frequency errors—transients, noises; and class D, yaw errors which are indirectly affecting the antenna pointing.

Yaw error effect is decomposed through some weighting into North-South and East-West errors, and added to the *A*, *B*, *C* resulting errors to give the North-South (NS) and East-West (EW) errors. Then an error cone is defined for the antenna pointing.

Performances in Normal and Station-Keeping Modes

The satellite comprises three antennae. One large antenna (30 kgm^2) with high pointing accuracy is capable of receiving RFS and APM, one offset antenna can be mounted on an APM in order to improve its pointing independency, and the third one is fixed. The main body (10,000 kgm^2) roll/pitch measurement is ensured by an IRES if not otherwise stated.

Five combinations of sensors and actuators have been analyzed in detail. In Configuration I, the three antennae are fixed and the large one incorporates an RFS used for main body attitude measurement. The main body is controlled by a 2-DOF system.

In Configuration II, the large antenna still uses an RFS for the main body. The second antenna receives an APM with low bandpass to improve its pointing by correcting biases through ground calibration. The main body is controlled by a 1 DOF (IIa) or 2 DOF (IIb) system.

In Configuration III, the main body is controlled through an IRES and a 2 DOF system. The second antenna has a low-bandpass APM. Calibration of the large antenna is done through the wheel system to correct biases.

In Configuration IV, the large antenna comprises a high-bandwidth APM and RFS. The second antenna also has a high-bandwidth APM. The central body is controlled through the RFS and a 1 DOF system. The error budgets are summarized in Tables 3 and 4. It should be noted that no flexibility problem has been taken into account in these budgets.

Conclusions

Use of RF sensors is of very significant interest for antenna pointing measurement. Measurement performance improvement of typically 0.1 deg (from 0.15 deg. to 0.05 deg.) can be obtained. Use of antenna pointing mechanisms is necessary only when several antennae need very accurate pointing. If only one antenna must be accurately controlled, the low bandwidth APM provides a limited performance improvement, compared with the 2-DOF control system for the other antennae. If flexibility problems are critical, the APM (HBW) use seems more favorable than the 2 DOF system, since it allows decentralized control.

Acknowledgment

The authors wish to especially thank CNES, which has sponsored part of the work presented in this paper.

References

[1]Broquet, J. and Govin, B., "Application of a One Degree of Transverse Freedom System to the Attitude Control of an Operational Ariane Large Satellite," ESA Conference on Attitude and Orbit Control System, ESA SP-128, Noordwijk, Oct. 3-6, 1977, pp.29-36.

[2]Bryson, A.E. Jr. and Kortum, W., "Estimation of Local Attitude of Orbiting Spacecraft," *Proceedings of Fourth IFAC Symposium on Automatic Control in Space*, Dubrovnik, Yugoslavia, Sept. 6-10, 1971.

[3]Hsing, J.C., Ramos, A., and Barret, M.F., "Gyro-Based Attitude Reference Systems for Communications Satellites," *Journal of Guidance, Control, and Dynamics*, Vol. 3, May-June 1980, pp. 351-7.

[4]Anstett P. and Govin, B., "Study of an Integrated Attitude Sensing System and Development of a Prototype," *Proceedings of the 8th Symposium on Automatic Control in Space*, Pergamon Press, Oxford, England, 1980, pp. 257-265.

[5]Skelton, R.E., Hughes, P.C., and Hablani, H.B., "Order Reduction for Models of Space Structure Using Modal Cost Analysis," *Journal of Guidance, Control, and Dynamics*, Vol. 5, July/Aug. 1982, pp. 351-357.

[6]Likins, P., Ohkami, Y., and Wong, C., "Appendage Modal Coordinate Truncation Criteria in Hybrid Coordinate Dynamics Analysis," *Journal of Spacecraft*, Vol. 13, Oct. 1976, pp. 611-617.

[7]Claudinon, B. and Govin, B., "Study of Digital Adaptive Control Technique for Flexible Spacecraft," MATRA Final Report, under ESA Contract No 4120/79/NL/AK(SC), Vélizy, France, 1981.

[8]Strunce, R.R. and Henderson, T.C., "Application of Modern Modal Controller Design to a Large Space Structure," *AIAA Symposium on Dynamics and Control of Large Flexible Spacecraft*, Blacksburg, Va, June 21-23, 1979, pp. 661-675.